ELSEVIER

Ceramics International 33 (2007) 969–978

CERAMICS INTERNATIONAL

www.elsevier.com/locate/ceramint

Synthesis and characterization of nano $MgAl_2O_4$ spinel by the co-precipitated method

M.F. Zawrah [a,*], H. Hamaad [b], S. Meky [b]

[a] National Research Center, Ceramics Department, Dokki, Cairo, Egypt
[b] Al-Azhar University, Faculty of Science, Chemistry Department, Nasr City, Cairo, Egypt

Received 22 June 2005; received in revised form 14 January 2006; accepted 27 February 2006
Available online 24 April 2006

Abstract

Magnesium aluminate ($MgAl_2O_4$) spinel powders were prepared by co-precipitation of stoichiometric amounts of magnesium and aluminum chlorides at 80 °C. Some sintering aids such as ZnO and MnO_2 were added in the form of chlorides during the precipitation to study their effect on densification. The co-precipitated materials were a mixture of Mg–Al double hydroxide with the presence of few amounts of gibbsite and brucite. After heat-treatment of the precipitated powders up to 1000 °C, a crystalline spinel powder was obtained. The presence of 0.5, 1, 2 and 3 wt.% of ZnO or MnO_2 as sintering aids increased sinterability after firing up to 1550 °C. The highest density was obtained for the samples containing 2 wt.% ZnO or 3 wt.% MnO_2 which reached about >94 and 96% theoretical density (TD), respectively. The mechanical properties increased by adding ZnO or MnO_2, an exception being the sample containing 0.5 wt.% of ZnO for which relatively smaller value were obtained.

Keywords: Nano-particle; Spinel; Sinterability; Properties; Co-precipitation

1. Introduction

A spinel is a ternary oxide whose chemical formula is AB_2O_4, where A represent a divalent metal cation that normally occupies a tetrahedral site and B represents trivalent metal cations that normally occupy the octahedral sites of a cubic packed crystal [1]. The unit cell of the 2–3 magnesium aluminate spinel ($MgAl_2O_4$) can be expressed as $Mg_8Al_{16}O_{32}$ in which the 32 oxygen anions are cubic closed packed. Such close packing provides 64 divalent tetrahedrally coordinated cation sites and 32 octahedrally coordinated trivalent cation sites, of which only 24 are filled. Therefore, the unit cell of the $MgAl_2O_4$ spinel is considered a host cell capable of holding a large number of divalent and trivalent cations in solid solution [1,2].

Magnesium aluminate spinel is a ceramic materials with good mechanical strength, thermal, chemical and optical properties which find applications in metallurgical, chemical, electro technical, catalysis and electronic industries [3–7]. Over the last few decades, a variety of techniques [8–11] have been used to prepare $MgAl_2O_4$ spinel. These include the hydrothermal technique, plasma spray decomposition of oxides, sol–gel, combustion of metal nitrated and urea, freeze drying of sulfate solutions, controlled hydrolysis of metal alkoxides decomposition of organometallic compounds in supercritical fluids, magnesium aluminum double alkoxide, and an aerosol method [12]. Dense materials of stoichiometric composition with high purity characteristics are difficult to fabricate directly from mixtures of individual Al_2O_3 and MgO powders via solid-state technique, since the volume expansion (5%) accompanying the spinellization reaction [13] is detrimental to densification. In practice, dense materials are produced by a two-stage firing process: calcining the powder mixture at ~1600 °C to complete the spinellization reaction, followed by ball milling and refiring at even higher temperatures.

The present investigation was undertaken to develop stoichiometric Mg–Al spinel powders from co-precipitated magnesium and aluminum double hydroxides. Attempts have been made to study the effect of ZnO and MnO_2 additives on the densification and properties of the magnesium aluminate spinel.

* Corresponding author. Fax: +20 2 3370931.
E-mail address: mzawrah@hotmail.com (M.F. Zawrah).

0272-8842/$32.00
doi:10.1016/j.ceramint.2006.02.015

2. Experimental procedures

2.1. Preparation of spinel powders

Mixed solution of stoichoimetric magnesium and aluminum chlorides with Mg^{2+}/Al^{3+} ratio of approximately 1:2 were prepared by dissolving the corresponding amount of magnesium and aluminum chlorides in 80 °C distilled water. Different ratios of zinc chloride or manganese chloride were added separately to obtain magnesium aluminate spinel containing 0.5, 1, 2 and 3 wt.% ZnO, or MnO_2 as additives. After mixing the corresponding chlorides, these solutions were stirred with excess of NH_4OH solution at pH 9.5–10.5. The gelatinous precipitate was kept at 80 °C for 1 h, cooled to room temperature, washed for several times by distilled water until free from chloride ions, and finally dried overnight at 110 °C [14].

2.2. Characterization of precipitated powders

The precipitated powders were characterized by thermogravimetric analyses (PERKIN-ELMER 7 Series Thermal-Analysis System) under the following conditions; static air, heating rate 10 °C/min, sample mass about 15 mg, reference sample Al_2O_3, and sensitivity of 40 μV. X-ray diffractometer (XRD, Siemens D500) was used to investigate the formed phases using Cu Kα radiation (λ = 0.1542 nm). The morphology of the precipitated powder was characterized using a transmission electron microscope (Zeiss type EM 10). Infrared spectra of the prepared powders were obtained using an URID automatic double beam infrared spectrophotometer in the range 4000–200 cm^{-1}.

2.3. Processing of MgO-Al_2O_3 ceramic bodies

Volume stable MgO–Al_2O_3 ceramic bodies containing 0.5, 1, 2 and 3 wt.% ZnO or MnO_2 were processed from the co-precipitated material by firing up to 1550 °C using a two stage firing process [15,16]. These batches were semi-dry pressed under 10 N/mm^2 into cubic samples of 2.5 cm edge length and subsequently calcined for 1 h at 1000 °C. The calcined briquettes were subsequently re-ground and repressed under 60 N/mm^2, using polyvinyl alcohol binder into cylindrical samples of 1.25 cm diameter and about 1.25 cm height. The pressed samples were finally dried and fired for 2 h up to 1550 °C to study the densification behavior and other properties of the fired bodies.

2.4. Densification of spinel bodies

The densification parameters of fired MgO–Al_2O_3 pellets were determined by means of bulk density (BD) and apparent porosity (AP) according to the Egyptian Standard No. 1859 (1990). The bulk density and apparent porosity of the fired samples were determined using the liquid displacement technique [17,18]. The method was based on soaking the fired samples under kerosene for 1h in vacuum desiccator. This method was adopted to prevent hydration of free MgO bearing phases. The phase composition of the fired spinel ceramics were qualitatively determined by XRD (Philips PW 1710 diffractometer) with Cu Kα radiation. Microstructure of the dense samples was investigated using a computerized SEM of a Joel JSM-T 330 scanning electron microscope. The mechanical properties in terms of cold crushing strength at room temperature were tested by using a PEZ 2979 machine with maximum load of 100 KN.

3. Results and discussion

3.1. Phase composition of precipitated powders

X-ray diffraction patterns of pure precipitated magnesium aluminate powders and those containing ZnO, or MnO_2, as additives are shown in Figs. 1 and 2. X-ray analyses show the co-precipitated hydroxide is a mixture of gibbsite [$Al(OH)_3$] and a Mg–Al double hydroxide (DH) [$2Mg(OH)_2{\cdot}Al(OH)_3$], with little amount of brucite [$Mg(OH)_2$]. The double hydroxide salt is one of a large family of layer lattice structures [19,20] that were shown by Feitknech [21,22] to form by the combination of divalent and trivalent ions of similar atomic radii.

The stability of the double hydroxides was suggested to be due, in part, to Cl^- ions that compensate for induced positive charges resulting from the substitution of Al^{3+} for Mg^{2+} ions. The importance of the formation of a double hydroxide in the present study is that spinel is a direct decomposition product after heat treatment [23–27].

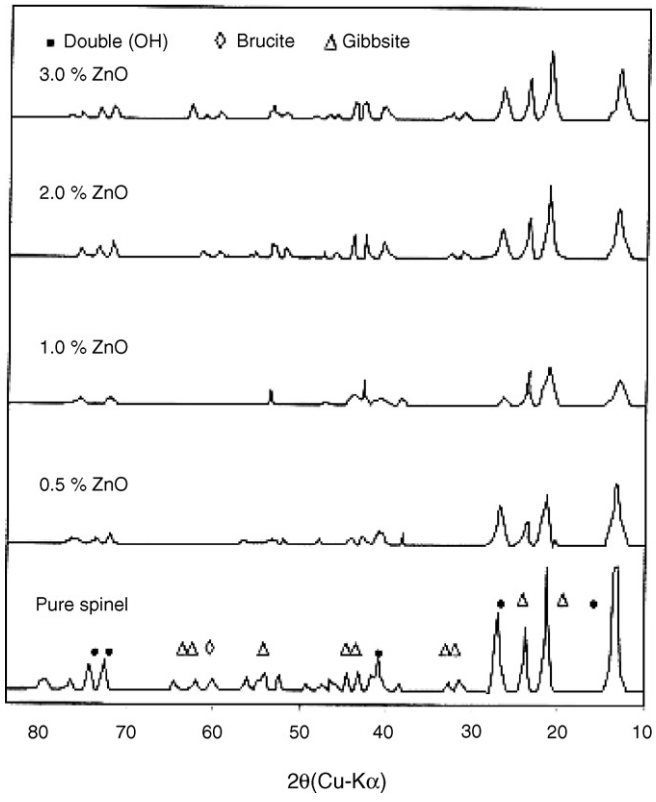

Fig. 1. XRD of pure precipitated Mg–Al spinel powders and those contain ZnO.

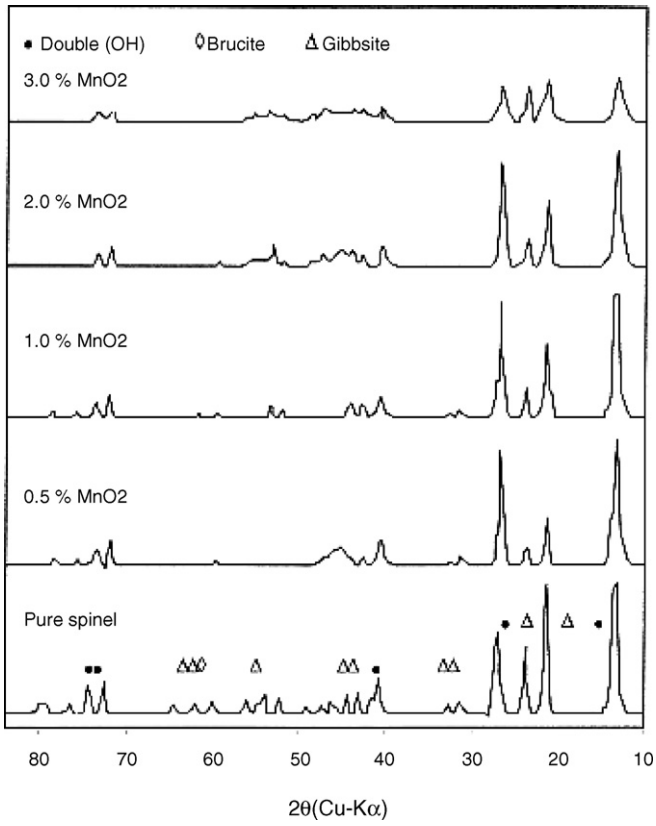

Fig. 2. XRD of pure precipitated Mg–Al spinel powders and those contain MnO_2.

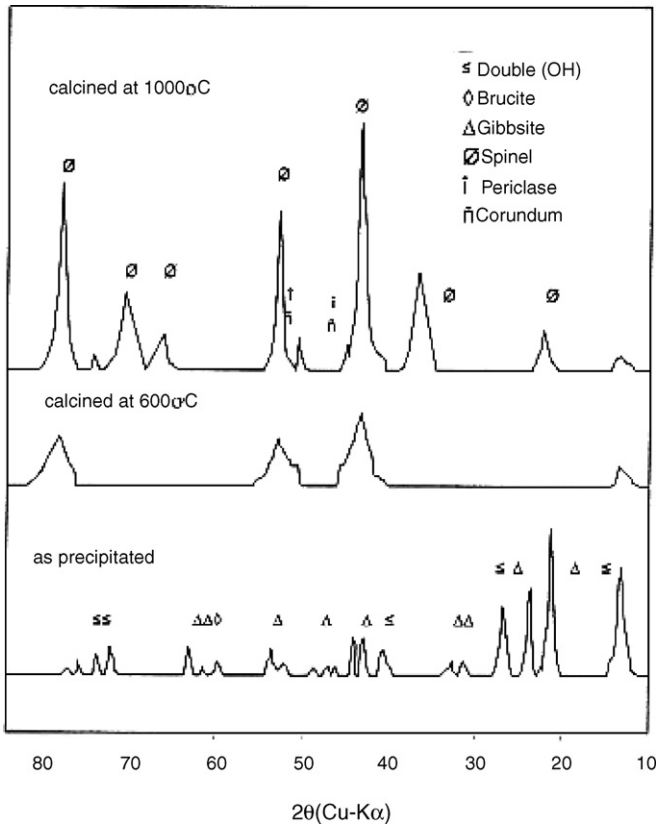

Fig. 3. XRD of the as prepared and the calcined pure Mg–Al spinel powders at 600 and 1000 °C.

Fig. 1 also shows that peak intensity of DH and gibbsite decreases with the increase of ZnO content reaching its minimum intensity with 1 wt.% and then increases again with higher ZnO content in spite of its intensity still much lower than that of pure spinel. Also, gibbsite peaks behave in the same trend. The peaks of brucite disappeared with the increase of ZnO and MnO_2 (Figs. 1 and 2).

Optimum calcination temperature needed to give well-crystallized spinel powders was investigated. XRD of the as prepared and the calcined pure spinel powders at 600 and 1000 °C are shown in Fig. 3. Calcination products of the precursor are essentially amorphous to X-rays at temperature lower than 600 °C. At 600 °C, broad peaks corresponding to spinel ($MgAl_2O_4$) and periclase (MgO), decomposed from the double hydroxide and brucite [$Mg(OH)_2$], appeared in the XRD patterns. Dominant formation of spinel started at >600 °C through solid-state reaction between periclase and a polymorph of alumina decomposed from the gibbsite or the double hydroxide. Due to high reactivity of γ-Al_2O_3 and MgO (decomposed from the double hydroxide) as well as their intimate mixing, complete conversion of the precursor to spinel was nearly achieved by calcination at 1000 °C, with only small amount of periclase detected [23,24,27,28]. Above 1000 °C, continued refinement in peak shapes and intensities were observed, indicating crystallite growth as the calcination temperature increases.

Figs. 4 and 5 show XRD of pure magnesium aluminate spinel as compared with those containing different amount of ZnO, and MnO_2 after calcination at 1000 °C. Peaks characterizing well-crystalline spinel phase appeared in all samples in addition to peaks of periclase detected in the pure magnesium aluminate and in samples containing 3 wt.% ZnO. Generally, the samples containing MnO_2 as additive show higher crystallinity than those containing ZnO.

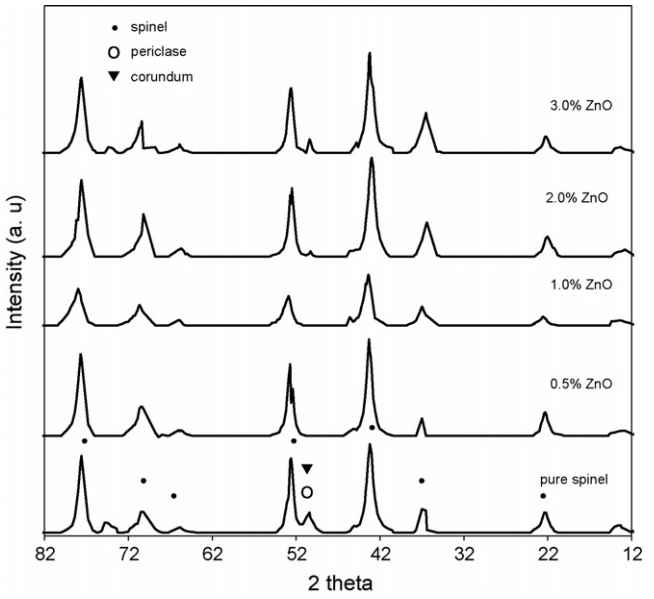

Fig. 4. XRD of pure Mg–Al spinel and those contain different amount of ZnO, after calcination at 1000 °C.

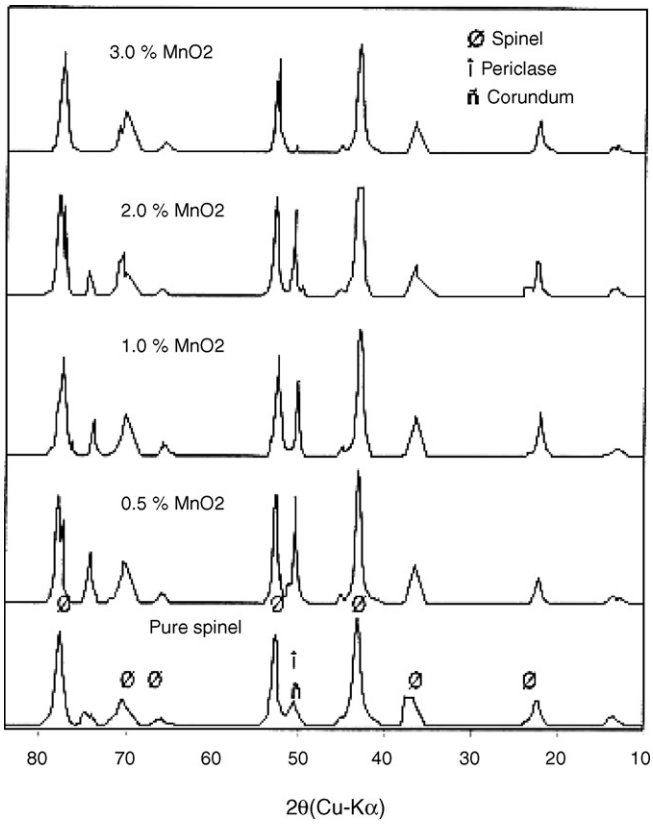

Fig. 5. XRD of pure Mg–Al spinel and those contain different amount of MnO_2 after calcination at 1000 °C.

In the TGA curves of pure magnesium aluminate, Fig. 6, three weight losses are noticeable with their maxima at temperatures of about 150, 280 and 600 °C. After the loss of free water or/and a small amount of residual ammonia adsorbed on the sample surface at 50–150 °C, the TG curve can be divided into three steps. The first one ends at about 220 °C. The second step (up to about 400 °C) starts slowly and then becomes faster. The last step, characterized by a decreasing weight-loss rate, is nearly completed at 650 °C. The weight loss located between 220 and 280 °C is due to the intermolecular water, but the other located between 300 and 450 °C corresponds to the dehydroxilation of the mixed hydroxides to oxides. The weight loss stages in TGA result in about 40% weight loss in total. Above 600–650 °C, no weight loss was observed in the TGA profile due to dissociation of all formed hydroxides before this temperature. This indicates that solid-state reaction to form $MgAl_2O_4$ spinel may occur above 600–650 °C [29–35].

From the thermal and X-ray data, and the well-known dehydration reactions exhibited by the hydroxides of magnesium and aluminum, a possible reaction sequence leading to the formation and crystallization of spinel may be proposed.

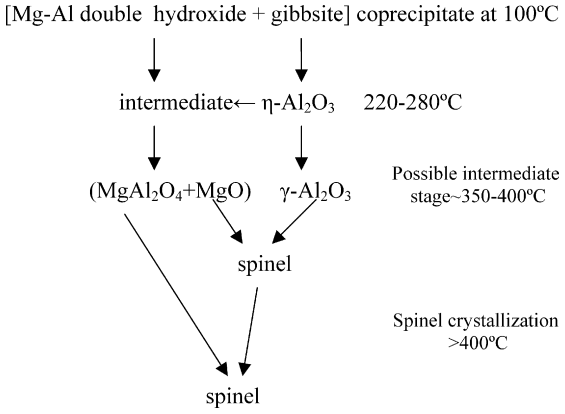

3.2. Infrared spectroscopy

Fig. 7 shows IR spectrum of precipitated pure Mg–Al hydroxide and their calcined powder at 600 and 1000 °C. IR spectrum indicates that the precipitated material is a hydrate. The strong broad band between 3150 and 3550 cm^{-1} and the band at 1650 cm^{-1} are evidence of molecular water in the structure. The former is associated with O–H stretching vibrations (symmetric and antisymmetric) in molecular water, while the latter is due to the H–O–H bending mode [36]. Their appearance at high temperatures up to 1000 °C is most probably due to inter absorption during the compaction of the powder specimens with KBr. The peaks between 700 and 1200 cm^{-1}

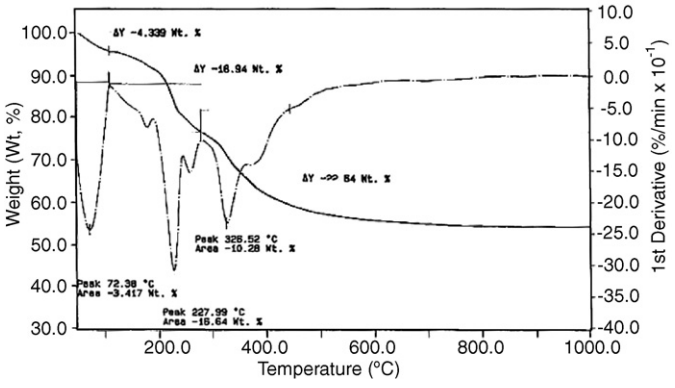

Fig. 6. TG thermogram of the precipitated pure Mg–Al spinel powder.

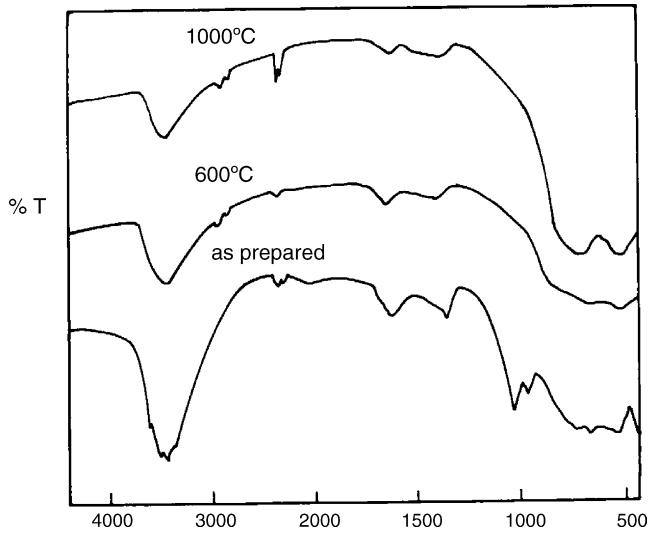

Fig. 7. IR spectra of the precipitated Mg–Al spinel powder at different firing temperature.

are due to the O–H bending mode. These peaks disappear with raising the calcination temperature up to 1000 °C. The small two peaks at 610 and 750 cm^{-1} are characteristic of boehmite as reported by Clarke and co-workers [37,38]. Also, they disappeared by increasing the calcination up to 1000 °C. After calcination at 600 °C, new small and broad two peaks at 631 and 511 cm^{-1} appeared due to AlO_6 group building up of spinel. Their area and intensity increase with raising temperature up to 1000 °C.

3.3. Morphology of the precipitated powder

Fig. 8 shows the particle size and morphology of the precipitated pure magnesium aluminate spinel. The slightly rough

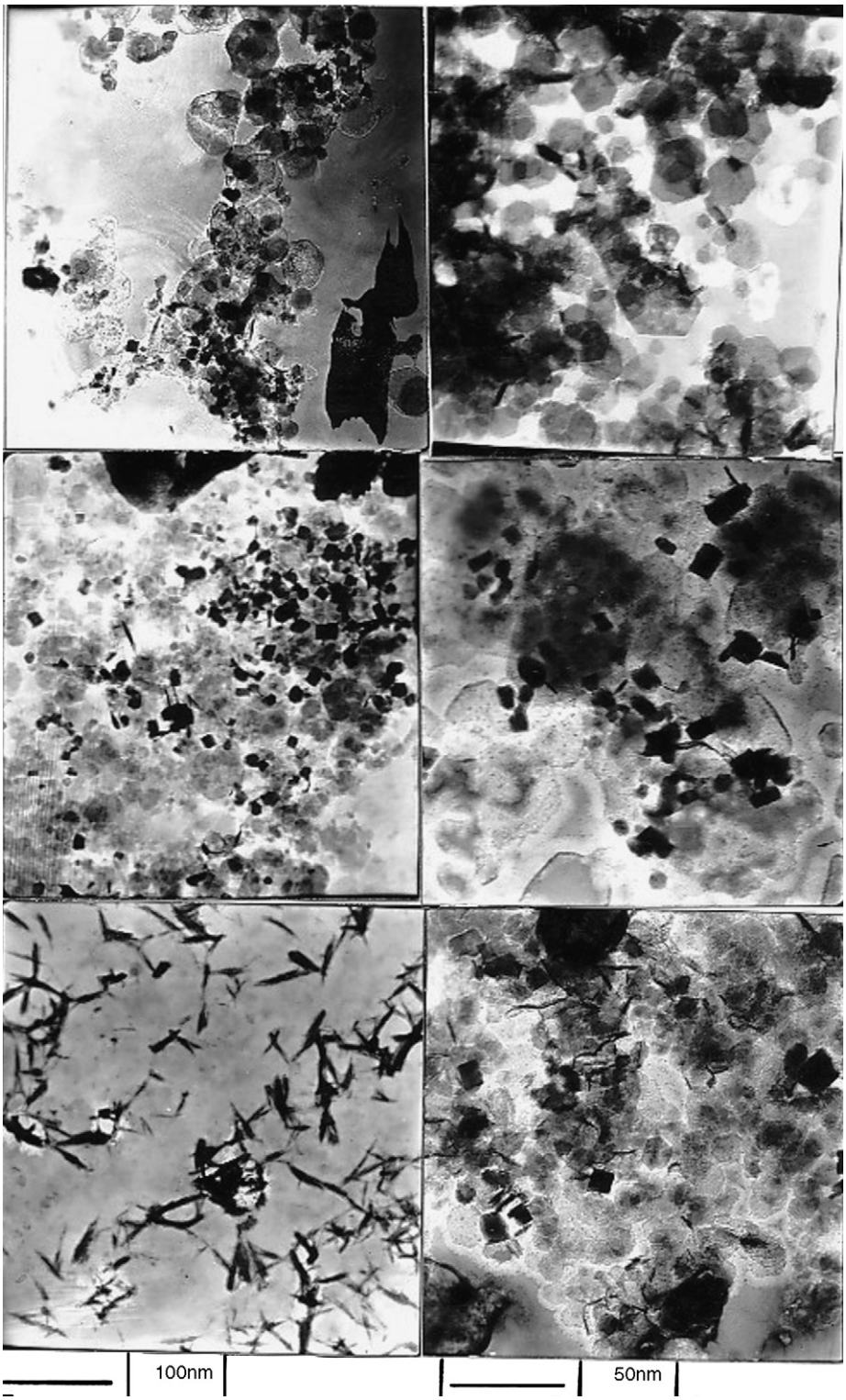

Fig. 8. TEM of the precipitated Mg–Al spinel powder.

surface indicates that these particles are essentially secondary agglomerates of finer grains. The micrograph showed different morphologies and their particle size varied in narrow different ranges. It was found that many fine cubic-type grains were formed when the samples were prepared by the co-precipitation method with either ammonia or ammonium carbonate used as precipitation agent [39,40]. The grain size distribution of the precipitated samples is in the range of about 25–60 nm.

As illustrated in Fig. 8, when this system contains a mixture of Mg^{2+} and Al^{3+} hydroxides with their polymorphism, different morphologies are obtained. Generally some grains exhibit a plate like shape with poorly defined edges. Also, well-defined cubic and rounded grains are observed. These seem to be the grains of Mg–Al double hydroxides. On the other hand, many different shapes with defined edges are observed. Hexagonal plates and hexagonal prisms of magnesium hydroxide appeared. Elongated fiber-like bundles or rounded particles characteristic of boehmite and gibbsite structures are also observed.

3.4. Densification of the prepared Mg–Al powders

The variation of bulk density and apparent porosity of spinels containing ZnO and MnO_2 with sintering temperature are shown in Figs. 9 and 10. Spinel without additive achieves a

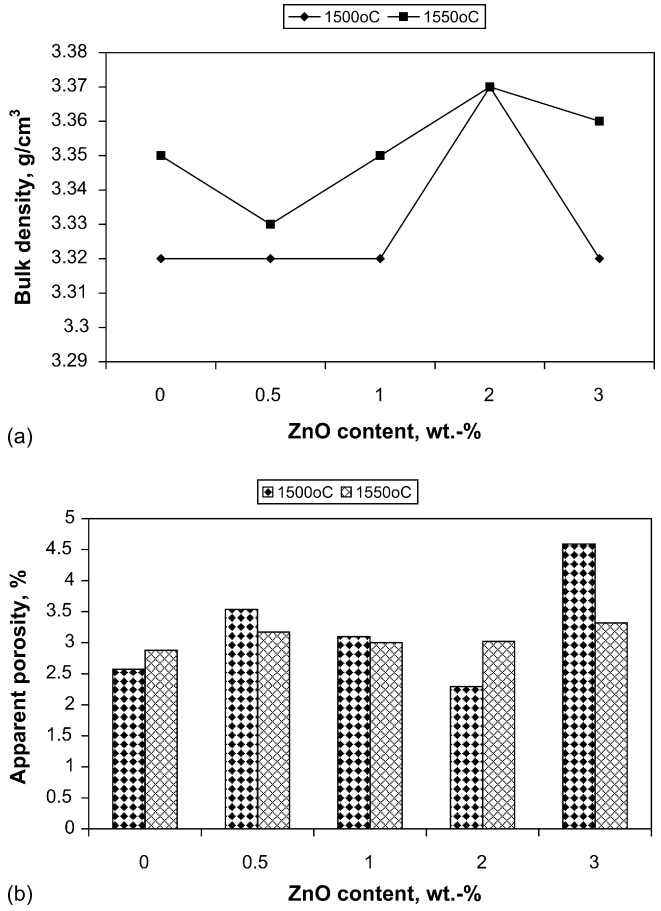

Fig. 9. Bulk density of and apparent porosity sintered Mg–Al spinel-containing ZnO.

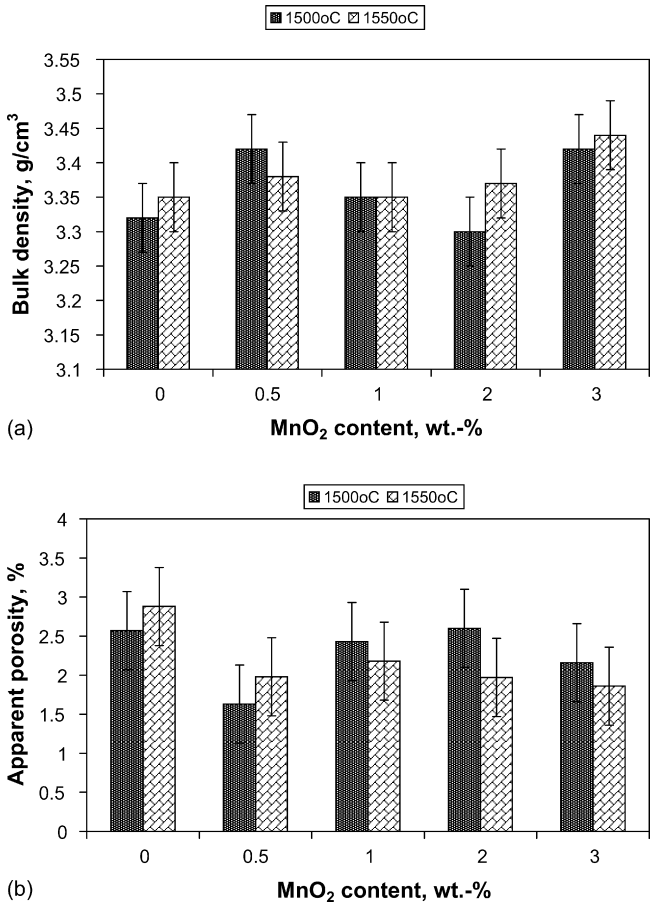

Fig. 10. Bulk density and apparent porosity of sintered Mg–Al spinel-containing MnO_2.

bulk density of 3.30–3.35 g/cm^3 at 1500 and 1550 °C, which is 92–94% of the theoretical density (TD) of magnesium aluminate spinel (3.58 g/cm^3). Bulk density of pure spinel gradually increases with sintering temperature up to 3.35 g/cm^3 (94% of RD) at 1550 °C. The behavior of densification was different in the case of ZnO- and MnO_2-incorporated Mg–Al spinel. The samples containing ZnO achieve their highest bulk density at 1550 °C with 2 wt.-% ZnO which thereafter decreases slightly. Samples containing MnO_2 behave in opposite way, their bulk density decreases with increasing of MnO_2 content, reaches its minimum value at 2 wt.% content and then increases up to the maximum bulk density value (3.44 g/cm^3 ≈96% TD) with 3 wt.% MnO_2. The ZnO additive was supposed to enter into the spinel structure and create anion vacancy in Al_2O_3 and thereby to favor the densification process. Nevertheless, when the amount of ZnO is higher (about 3 wt.%), the density decreases marginally. Though the substitution of ZnO in spinel creates anion vacancy, as it is not fully soluble, the excess ZnO remained in the grain boundary. Therefore, it hindered the boundary migration, which may be the cause of the decrease in density.

The spinel samples containing MnO_2 show generally a better bulk density than those containing ZnO additive. The influence of manganese oxide addition was shown to accelerate the sintering rate and grain growth. Similar to the effect of TiO_2, the

sintering rate is high at 0.5 wt.% and then levels off and starts decreasing as the MnO_2 concentration exceeds 0.5 wt.% presumably due to the formation of a second phase [41–43].

Concerning the sintering of spinel by MnO_2 addition, Mn occupying a cation site increases the oxygen ion vacancy concentration. A gradient in Mn concentration results in a wide region of enhanced diffusion at the grain boundaries. The relatively low bulk density at 1 and 2 wt.% additives seems to be due to grain growth. However, MnO_2 is known is greatly enhance grain growth [44].

It is evident that the density of these ceramic bodies is generally higher than the literature data for materials densified at 1700 °C [45,14,15]. This is mainly due to the very fine particles (size 25–60 nm) and the homogeneity of our calcined co-precipitates.

In addition, the bulk density of pure spinel and samples containing MnO_2 are higher than those containing ZnO, due to the presence of excess MgO than that required for spinel formation, which enhances the sintering of spinel.

3.5. Phase composition of the sintered spinel bodies

Fig. 11 shows XRD patterns of the co-precipitated pure $MgAl_2O_4$ spinel as well as those containing ZnO_2 and MnO_2 after firing at 1550 °C for 2 h. It can be seen that pure spinel and that containing MnO_2 are mainly composed of spinel solid solution and periclase (MgO) with higher periclase concentration in pure spinel. Whereas ZnO_2-containing spinel was composed of spinel solid solution only. As a result of the formed spinel solid solution, the diffraction lines of the phase are slightly shifted about 0.2 Å.

3.6. Microstructure of the sintered spinel bodies

Figs. 12a–b and 13a–d show the photomicrographs of the sintered magnesium aluminate spinel and the ones containing ZnO additive sintered at 1550 °C for 2 h respectively. All spinel grains appear rounded or equiaxed in shape with higher degree of direct bonding except that containing 1.0 wt.% ZnO (Fig. 13b) which shows euhedral direct-bonded spinel grains

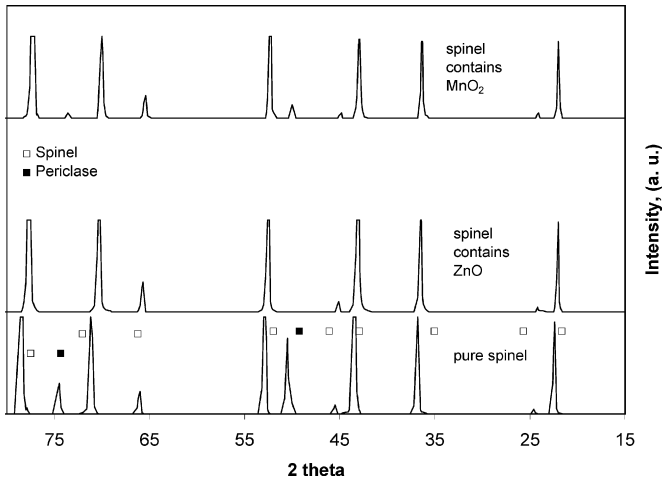

Fig. 11. XRD of sintered Mg–Al spinels.

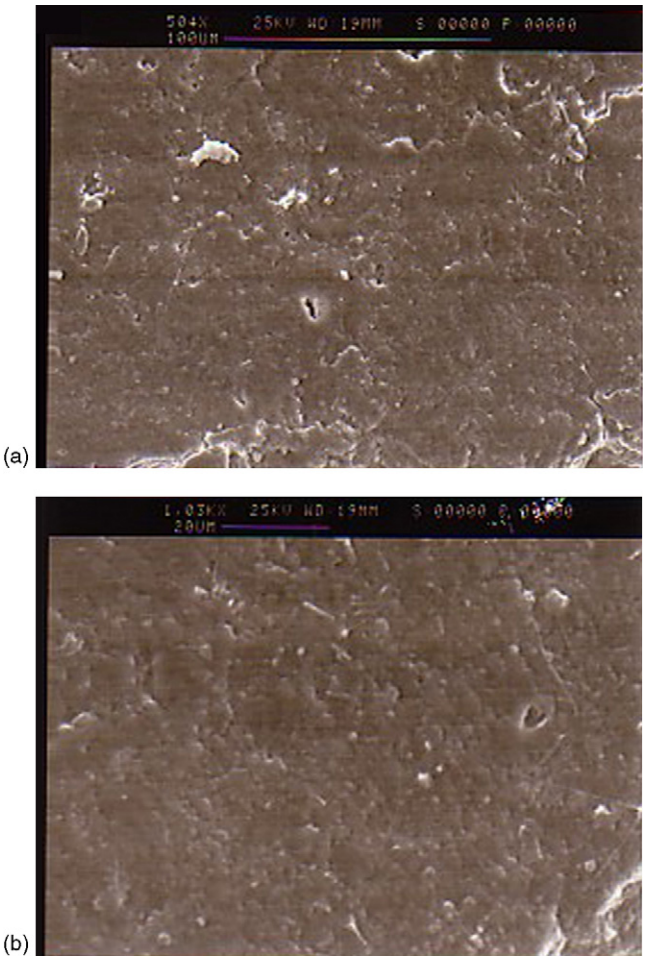

Fig. 12. Microstructure of sintered pure spinel.

and larger grain growth (5–10 μm). The grain sizes of the samples containing 0, 0.5, 1, 2, 3 wt.% ZnO are about 1–3 μm. All samples show very low intragranular pores. Ghosh et al. [46] found that in magnesium aluminate spinel containing 2 wt.% ZnO as additive, 1.25 wt.% goes into the Mg–Al grains by solid solution. Therefore, it is supposed the extra ZnO remains between the grains and acts as a barrier for boundary movements and restricts grain growth. This microstructure is homogeneous, with high-density crystalline zones surround by low-density areas and pore clusters. Because the prepared spinel powder had a small primary crystal size and a large specific surface area, shrinkage was likely to occur readily during sintering and large pores were trapped. The photomicrograph of magnesium aluminate spinel grains containing 0.5, 1, 2, and 3 MnO_2 are shown in Fig. 14a–d. It appears that this microstructure is denser and finer than for ZnO as additive. The grain sizes are about 1–2 μm in samples containing 0.5 and 1 wt.% ZnO, while it is around 3–9 μm for the samples contain 2 and 3 wt.% MnO_2. The photomicrograph of the sample containing 0.5 wt.% MnO_2 is homogeneous with rounded and well defined direct-bonded spinel-spinel grains, while those containing 1, 2 and 3 wt.% are relatively heterogeneous with some rounded or undefined grain boundaries direct-bonded together. As shown in Fig. 14a 0.5 wt.% MnO_2 addition led to inhomogeneous grain growth after sintering at 1550 °C for 2 h,

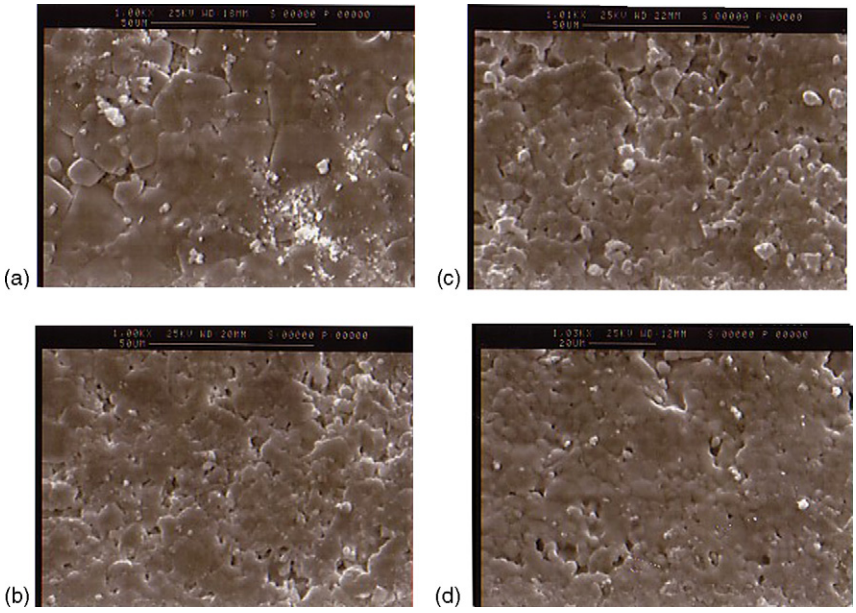

Fig. 13. Microstructure of sintered Mg–Al spinel-containing ZnO.

resulting in a microstructure with localized regions of finer grains around lager sized grains. Intergranular grain boundary phase was detected between the grains as a thin layer in samples with 2–3 wt.% MnO_2 sintered at 1550 °C for 2 h. Based on these observations, the volume or grain boundary diffusion mechanism acts as the controlling process according to the composition and the sintering conditions during the later stages of densification [47].

3.7. Mechanical properties

Mechanical behavior of spinel and ceramic materials at room as well as high temperature has been reported in the literature [47–52]. The mechanical properties in terms of cold crushing strength (CCS) of the sintered spinel containing ZnO or MnO_2 are shown in Fig. 15. Generally, cold crushing strength increases by adding ZnO or MnO_2 except for the sample containing 0.5 wt.% ZnO which gives relatively smaller value. It was found that the strength increases with the increase of the amount of ZnO reaching its maximum value with 3 wt.% ZnO i.e. 137 MPa. The minimum strength was noticed with 0.5 wt.-% ZnO. Addition of ZnO from 1 to 3 wt.% improves the strength, due to higher density and lower porosity. Related to the spinel that contains MnO_2, above 2 wt.%, the strength reduced to 105 MPa, which was still higher than that of spinel without MnO_2. In this sample, the excess MnO_2 remains in the

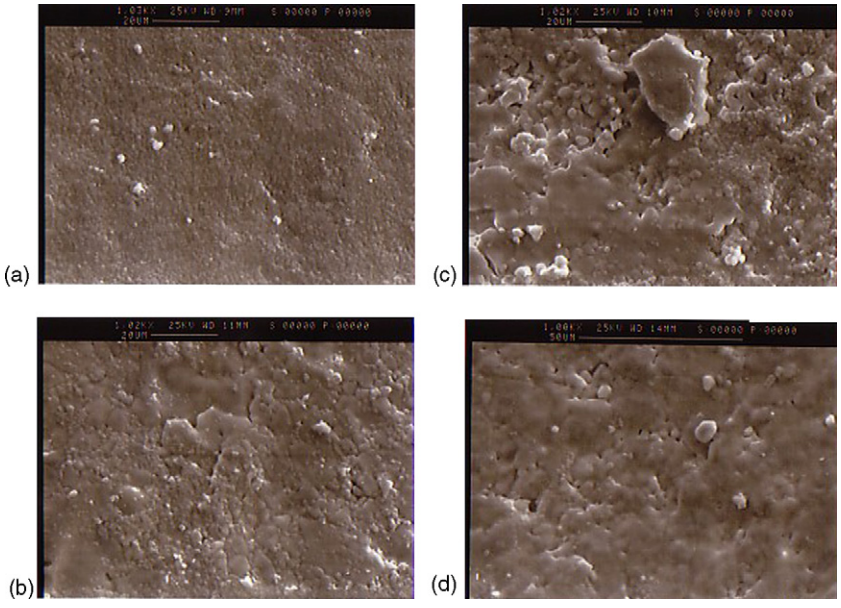

Fig. 14. Microstructure of sintered Mg–Al spinel-containing MnO_2.

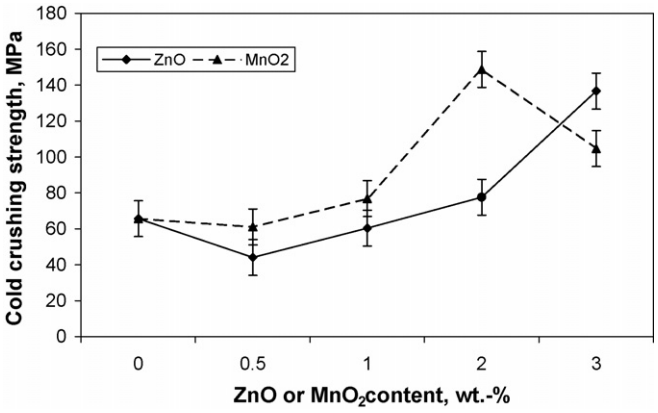

Fig. 15. Mechanical properties of sintered Mg–Al spinels.

grain boundary, thereby weakening the structure and hence the strength.

4. Conclusions

The co-precipitated spinel powders were a mixture of Mg–Al double hydroxide with the presence of few amount of gibbsite and brucite with 25–60 nm particle size. After their heat-treatment up to 1000 °C, crystalline spinel powder was obtained. Bands in IR spectra corresponding to the existence of AlO_6 groups prior to magnesium spinel formation, which was the only crystalline phase at 1000 °C, were observed. The presence of 0.5, 1, 2 and 3 wt.% of ZnO or MnO_2 as sintering aids for stoichoimetric spinel lead to the increase of sinterability after firing up to 1550 °C. The highest density was for the samples containing 2 wt.% ZnO or 3 wt.% MnO_2 which reached about >94 and 96 TD, respectively. The mechanical properties increased by adding ZnO or MnO_2 except for the sample containing 0.5 wt.% ZnO which gave relatively smaller values.

The present work showed that nanocrystalline magnesium aluminate spinels which are usually obtained from the sol–gel technique with expensive metallorganic compounds, can be prepared by using the traditional coprecipitation method with low cost chemicals.

References

[1] Edwin H. Wallker Jr., Jhon Wesley Owens, Marcus Etinne and Don walker, Mater. Res. Bull. 37 (2002) 1041–1050.
[2] M.A. Serry, S.M. Hammad, M.F.M. Zawrah, Br. Ceram. Trans. 97 (6) (1998) 175–178.
[3] L.B. Berry, B. Mason, R.V. Dietrich, Mineralogy: Concepts, Description and Determinations, second ed., W.H. Freeman and Germany, San Francisco, CA, 1983.
[4] Ranjan K. Pati, Panchanan Prmanik, J. Am. Ceram. Soc. 83 (7) (2000) 1822–1824.
[5] P. Pramanik, Chemical synthesis of nanosized oxides, Bull. Mater. Sci. 19 (6) (1996) 957–961.
[6] J. Salmons, J.A. Galicia, J.A. Wang, M.A. Valenzuela, Aguilar-Rios, J. Mater. Sci. Lett. 19 (2000) 1033–1037.
[7] J.I. DI Cosimo, C.R. Apesteguia, M.J. Gines, E. Iglesia, in: Proceedings of the 16th Meeting of North American Catalysis Society, May 30–June 4, 1999. Boston, USA, Technical Program, p. 60.
[8] J.J. Alcaraz, B.J. Arena, R.D. Gillespie, J. Holmgren, in: Proceedings of the 15th Meeting of North American Catalysis Society, May 30–June 4, 1997. Chicago, USA, Technical Program, p. 114.
[9] M. Barj, J.F. Bocquet, J.K. Chhor, C. Pommier, J. Mater. Sci. 27 (1992) 2187–2192.
[10] C. Pommier, J.K. Chho, J.F. Bocquet, M. Barj, Mater. Res. Bull. 25 (1990) 213–221.
[11] O. Varier, N. Hovanain, A. Larbat, P. Bergez, L. Cot, J. Chapin, Mater. Res. Bull. 29 (1994) 479–488.
[12] N. Yang, L. Chang, Mater. Lett. 15 (1992) 165–171.
[13] H. Erkalla, Z. Misirh, M. Demirci, C. Toy, T. Baykara, J. Eur. Ceram. Soc. 15 (1995) 165–171.
[14] Ji-Gug Li, Takaysu Ikegami, Jong-Hean Lee, Toshiyuki Mori, Yoshiyki Yajima, Ceram. Int. 27 (2001) 481–489.
[15] M.F. Zawrah, M.A. Serry, K.-H. Zum Gahr, cfi/Ber. DKG 76 (5.) (1999).
[16] M.A. Serry, M.F. Zawrah, R. Telle, cfi/Ber. DKG 75 (3.) (1998).
[17] M.F. Zawrah, M.A. Serry, J. Schneider, K.-H. Zum Gahr, cfi/Ber. DKG 77 (3) (2000).
[18] J.H. Chesters, Refractory, Production and Properties, Iron and Steel Institute, London, 1973.
[19] K. Shaw, Refractories and their Uses, Applied Science Publisher, London, 1973.
[20] Ji-Guang Li, Takayasu Ikegami, Jung-Heun Lee, Toshiyuki Mari, Yoshiyuki Yajima, Ceram. Int. 27 (2001) 481–489.
[21] M.J. Hudson, S. Carlino, D.C. Apperley, J. Mater. Chem. 5 (2) (1995) 323–329.
[22] W. Feitknech, Helv. Chim. Acta 25 (1942) 555–565.
[23] W. Feitknech, Gerber, Double Hydroxides And Basic Salts III (1942) 131–137.
[24] R.J. Barton, Ceram. Bull. 48 (8) (1969) 759–762.
[25] J. Katanic-popvic, N. Miljevic, S. Zec, Ceram. Int. 17 (1991) 45–52.
[26] O. Xamaguch, H. Omaki, K. Shimizu, J. Jpn. Soc. Powder Powder Metell. 22 (6) (1975) 202–204.
[27] S. Hokazono, K. Manako, A. Kato, Br. Ceram. Trans. 91 (1992) 77–79.
[28] T. Shiono, K. Shiono, K. Miyamoto, G. Pezzotti, J. Am. Ceram. Soc. 23 (1) (2000) 237.
[29] K. Hayashi, S. Toyoda, K. Morinaye, J. Ceram. Soc. Jpn. 99 (t) (1991) 550–555.
[30] G. Gusmano, P. Nunziante, E. Traversa, G. Chiozzini, J. Eur. Ceram Soc. 7 (1991) 31–39.
[31] O. Yamaguchi, H. Taguchi, Y. Miyata, M. Yohinaka, K. Shimizu, Polyhedron 6 (1987) 1587–1592.
[32] G. Mascolo, O. Marino, Miner. Mag. 43 (1980) 619–621.
[33] C.W. Beck, Amr. Miner. 35 (1950) 985–1013.
[34] F.A. Mumpton, H.W. Jaffe, C.S. Thompson, Am. Miner. 50 (1965) 1893–1913.
[35] W.T. Reichle, S.Y. Kang, D.S. Everhard, J. Catal. 101 (1986) 352–359.
[36] M.A. Ulibarri, C. Barriga, J. Cornejo, Thermochim. Acta 135 (1988) 231–236.
[37] D.S. Michael, T. Tseung-Yuen, L. soo, Ceram. Bull. 63 (2) (1984) 301–309.
[38] D.E. Clarke, J.J. Lannutt, Phase transformation in sol–gel derived aluminas, in: L.L. Tlench of, D.R. Ulrich (Eds.), Ultrastrudure Processing Of Ceramics, Glasses And Composites, John Wiely of Sons, New York, 1984 p. 126.
[39] J.A. Gadsden, Infrared Spectra of Mineral and Related Inorganic Compounds, Wiley, New York, 1978, p. 53.
[40] H. Nagia, S. Hokazono, A. Kato, Br. Ceram. Trans. J. 90 (1991) 44–48.
[41] J. Salmones, J.A. Galiea, J.A. Wang, M.A. Valenzuela And, G. Aguilar-Rios, J. Mater. Sci. Lett. 91 (2000) 1033–1037.
[42] Ritwik Sarkar, S.K. Das Banergee, Ceram. Int. 29 (2003) 55–59.
[43] J. Yu, K. Hiragashi, Taikabutsu Overseas 16 (4) (1994) 61;
J. Yu, K. Hiragashi, Taikabutsu Overseas 19 (4) (1999) 10–14.
[44] I.B. Cutler, Nucleation and nuclei growth in sintered alumina, in: W.D. Kingery (Ed.), Kinetics of High Temperature Processes, MIT Press, Cambridge, MA, 1959, pp. 120–127.
[45] P. Reynen, C. Zografou, D. vonMallinckrodt, Interceram, No. 2, 40-42, No. 3, 37-39, and No. 5, 40–43 (1983).

[46] A. Ghosh, K.W. White, M.G. Jenkins, A.S. Kobayashi, Bradt, J. Am. Ceram. Soc. 74 (1991) 1624.
[47] W.D. Kingery, H.K. Bowen, D.R. Ublman, Introduction to Ceramics, second ed., John Wiley and Sons, 1976 P479.
[48] W.B. Hilling, J. Am. Ceram. Soc. 76 (1) (1993) 129.
[49] R.L. Stewart, R.C. Bradt, J. Am. Ceram. Soc. 63 (1980) 619.
[50] M. Sakai, R.C. Bradt, A.S. Kobayashi, Nippon Seramikkasu Kyokai Gakujutsu Ronbunshi 96 (1988) 525.
[51] J.C. Hay, K.W. White, J. Am. Ceram. Soc. 76 (1998) 1849.
[52] K.W. White, G.P. Kelkar, J. Am. Ceram. Soc. 74 (1991) 1732.